

MECSOL 2019 - Analytical Modeling of Stresses in Steel Structures Considering Heat Transfer Phenomena

Tamires Martins Luiz ¹, and Luis Renato Chiarelli ¹

¹ Integrated Maria Imaculada Colleges, Paula Bueno, 240 – Centro, Mogi Guaçu – SP, 13840-040

Abstract: The temperature variation on the materials causes variations in its dimensions (displacement) which in turn causes additional stress in the structure. In some cases, these stresses can be significantly high and can cause several damages or even rupture in the structure. Metallic materials are relatively more susceptible to the thermal expansion when compared to concrete and this work evaluated the influence of heat transfer due to convection and radiation a metallic bridge by analytical models. Along the work different models of convection are verified with experimental results. Results showed that radiation had significantly more influence than convection in the variation of temperature and the models presented a temperature on the surface of the material around 375% and 281% higher than the ambient temperature. The relative error of the measured temperature and the calculated was around 38% and 12%. The variation in the forces were 888% and 667% of compression stress in the most requested bar.

Keywords: steel structures, solar radiation, temperature, stresses, experimental measurements

INTRODUCTION

The temperature variation on any material can cause variation in its dimensions, there may be dilation when there is an increase in temperature and contraction as it decreases. When the section of a structure is designed to sustain for this temperature oscillation and dilates uniformly, there is no stress; however, when there is an increase in temperature and the material does not dilate, there is thermal stress.

Direct solar radiation provides thermal energy to the structures and sun-lighted parts of structure become warmer and larger. Temperature difference on the lighted part of an object and on its shaded part leads to non-uniform deformations, curving of axes, occurrences of buckling, and in statically indeterminate systems these differences cause significant inner forces (Kordun (2015)). Along the last decades several heat transfer models which included conduction, convection and solar radiation were developed in order to help the engineers to design and evaluate their projects considering heat transfer, but these models usually are differential equations and the engineer must use numerical methods or software to approximate it. Considering the importance of temperature variation, this paper evaluates analytical models to determine the temperature variation without the use of computational resources. A steel bridge in Brasil, Mogi Guaçu/SP region is studied, and the thermal stress was calculated considering heat gain from solar radiation and loss of heat by the convection of the wind and radiation emitted Fig.1.

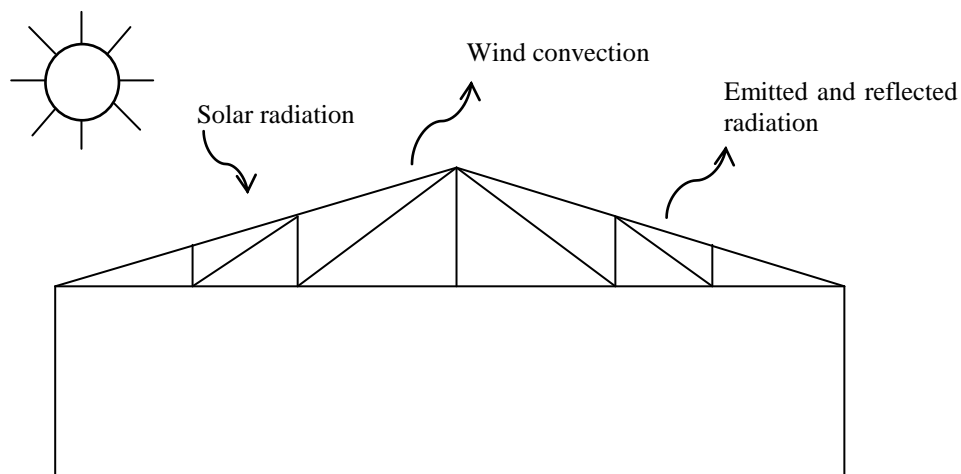


Figure 1 – Heat exchange actions in the trusses.

Heat exchange processes

Solar Radiation

Radiation is the energy emitted by matter at a non-zero temperature. Materials can absorb and emit radiation at the same time, this work adopted the ASHRAE clear sky model proposed in Liu, Chen and Zhou (2013). The value of the solar constant does not consider the absorption and scattering of the earth's atmosphere, which can be significant even on clear days (McQuiston, Parker and Spittle (2005)). The solar irradiation at the surface of the earth on clear days is given by:

$$G_{ND} = \frac{A}{\exp(B/\sin \beta)} C_N \quad (1)$$

where G_{ND} is the normal direct radiation (W/m^2), A is the apparent solar radiation at air mass equal to zero (W/m^2), B is the atmospheric extinction coefficient, β solar altitude and C_N the clearness number, $\sin \beta$ is calculated:

$$\sin \beta = \cos l \cosh \cos \delta + \sin l \sin \delta \quad (2)$$

with l representing the latitude that is commonly used on globes and maps, h is the angle between the equatorial plane and the projection on that plane of a line from the center of the earth, one hour of time corresponds to 15° of hour angle where the hour angle is negative in the morning and positive in the afternoon defined in Fig. 2.

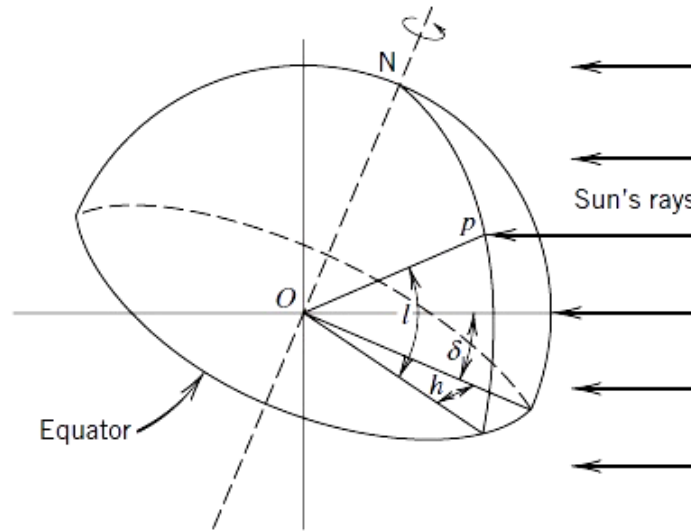


Figure 2 – Latitude, hour angle, and sun's declination (McQuiston, Parker and Spittle (2005)).

To find h it's necessary to calculate the solar hour LST through the formula:

$$LST = Local Standard Time - (L_L - L_S)(4 \text{ min/deg } W) + EOT \quad (3)$$

with $Local Standard Time$, the hour of the day considering the local daylight time DST , LL local longitude, LS standard meridian and EOT given by:

$$EOT = 229.2(0.000075 + 0.001868 \cos N - 0.032077 \sin N - 0.0014615 \cos 2N) \quad (4)$$

A where $N = (n-1)(360/365)$, being n the day of the year, δ is the angle between a line connecting the center of the sun and the earth and can be determined in degrees by the following:

$$\delta = 0.3963723 - 22.9132745 \cos N + 4.0254304 \sin N - 0.3872050 \cos 2N + 0.05196728 \sin 2N - 0.1545267 \cos 3N + 0.08479777 \sin 3N \quad (5)$$

On a surface arbitrary orientation, the direct radiation for clearness is calculated:

$$G_D = G_{ND} \max(\cos \theta, 0) \quad (6)$$

with θ the angle of incidence between the sun's rays and the normal to the surface. If $\cos\theta$ is smaller than zero, there is no direct radiation incident on the surface, $\cos\theta$ is:

$$\cos \theta = \cos \beta \cos \gamma \sin a + \sin \beta \cos a \quad (7)$$

γ is the surface solar azimuth and α is the tilt angle between the normal to the surface and the normal to the horizontal surface. Then a flat roof has a tilt angle of zero, and a vertical wall has a tilt angle of 90° as shown in Fig. 3.

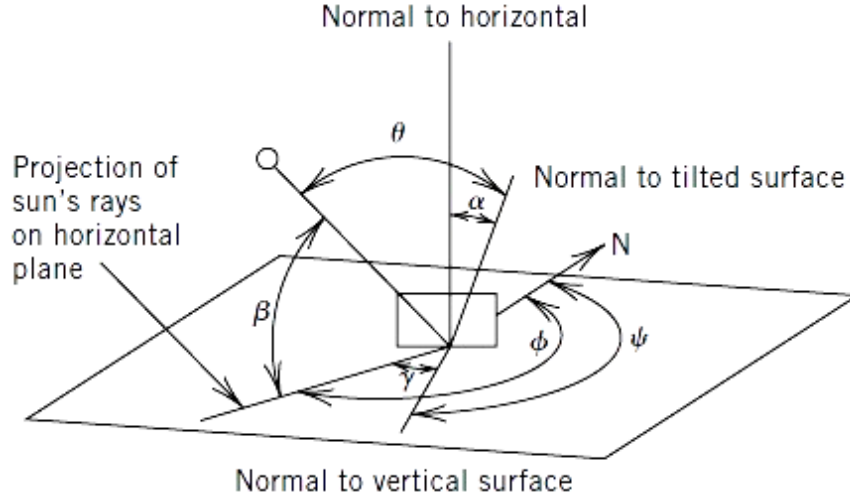


Figure 3 – Surface Solar Azimuth γ , Surface Azimuth ψ and Angle of Tilt α for an Arbitrary Tilted Surface (McQuiston, Parker and Spitler (2005))

The diffuse radiation on a non-horizontal surface can be found:

$$G_d = CG_{ND}F_{ws} \quad (8)$$

where C is the ratio of diffuse irradiation on a surface to direct normal radiation, F_{ws} the angle factor between the surface and the sky is:

$$F_{ws} = \frac{1 + \cos a}{2} \quad (9)$$

G_{dV}/G_{dH} is obtained:

$$\frac{G_{dV}}{G_{dH}} = 0.55 + 0.437 \cos \theta + 0.313 \cos^2 \theta \quad (10)$$

Eq. (10) can be calculated as Liu, Chen and Zhou (2013) proposes. In order to estimate the total rate at which radiation strikes a non-horizontal surface at the any time, the model also consider the energy reflected from the ground or surrounding onto the surface. The reflected radiation incident G_R on the surface can be calculated:

$$G_R = (G_D + G_{d\theta})\rho_g F_{wg} \quad (11)$$

with G_R the rate at which energy is reflected onto the surface (W/m^2), ρ_g is the reflectance of ground or horizontal surface, F_{wg} the configuration or angle factor from surface wall to ground obtained by:

$$F_{wg} = \frac{1 - \cos a}{2} \quad (12)$$

The total solar radiation is a function that depends of the solar absorption coefficient ε and radiation incident on a non-vertical surface:

$$q_s = \varepsilon(G_D + G_d + G_R) = \varepsilon \left[\max(\cos \theta, 0) + \frac{G_{dV}}{G_{dH}} C + \rho_g F_{wg} (\sin \beta + C) \right] G_{ND} \quad (13)$$

Long Wave Radiation

The long wave radiation on the surface of steel plates can be expressed by Stefan-Boltzmann model:

$$q_s = \varepsilon_f \sigma (F_{wg} (T_g^4 - T^4) + F_{ws} (T^4 - T_{sky}^4)) \quad (14)$$

where ε_f is the ratio of the radiation emitted by a surface; σ is Stefan-Boltzmann constant [$5.67 \times 10^{-8} \text{W}/(\text{m}^2 \cdot \text{K}^4)$], T_{sky} is the effective temperature of sky, usually calculated by $T_a - 6$ being T_a the ambient temperature, T_g is the ground temperature.

According to Liu, Chen and Zhou (2013) the ambient temperature is a critical parameter affecting the steel temperature. If the temperature data is not available, it can be estimated by:

$$T_a(t) = T_{av} + T_{am} \sin \frac{(t - t_0)\pi}{12} \quad (15)$$

with T_{av} the daily mean temperature, T_{am} is the amplitude and t_0 is the time when the maximum temperature occurs.

Convection

Convective heat transfer may occur through random molecular (diffusion) or through global movement or fluid macroscopic. The heat transfer rate by convection is given by Yazdani and Klems:

$$h = \sqrt{[C_t (\Delta T^{1/3})]^2 + [a V_0^b]^2} \quad (16)$$

where C_t is the turbulent natural convection constant, ΔT is the temperature difference between the exterior surface and the ambient air, a , b is the constants and V_0 is the wind speed at standard condition.

According to Danoso (2005) the natural convection coefficient of air for a vertical plate or wall is:

$$h = 1.77 (\Delta T)^{1/4} \quad (17)$$

Thermal stress calculation

Thermal stress is the additional stress caused by temperature increase or decrease. This stresses is considered normal, being of compression when there is temperature increase and traction when there is decrease. For the calculation of the thermal displacement is defined by Hibbeler (2009):

$$\partial_T = \alpha \Delta T L \quad (18)$$

∂_T is the total variation of the bar length, α is the linear expansion coefficient, ΔT is the temperature variation, L is the initial length.

Considering the bar set, the axial force of thermal origin in the bar is given by:

$$P_T = - \frac{\partial_T A E}{L} \quad (19)$$

with E the elasticity coefficient of the material. The thermal stress can be calculated:

$$\sigma_T = \frac{P_T}{A} = \frac{\partial_T E}{L} = -\alpha \Delta T E \quad (20)$$

Buckling

A Buckling analysis consists of determine the maximum load a structure can support before it collapses. The buckling was determined by the Euler's critical load formula:

$$P_{cr} = \frac{\pi^2 EI}{(KL)^2} \quad (21)$$

where P_{cr} is Euler's critical load, I the minimum area moment of inertia of the cross section of the column, L the unresponsive length of column and K the column effective length factor.

CASE STUDY



Figure 4 – Case study. Bridge (left) and thermometer (right) (Marques (2015)).

The bridge was constructed of steel alloy of iron for train passage and is over a hundred years old. It has a length of 35.6m and 60m considering the passages at each end. Its maximum height reaches about 3.628 meters and its width reaches about 5.5 meters as shown in Fig. 5 and 6. The bridge is bi-supported and to compute its loads was considered the weight of each element and the accidental load on the bridge slab corresponding to the crowd of people, for the calculation of the efforts was used the nodal equilibrium and the results are given according to Tab. 1 proposed by Marques (2015) and Pereira (2015).

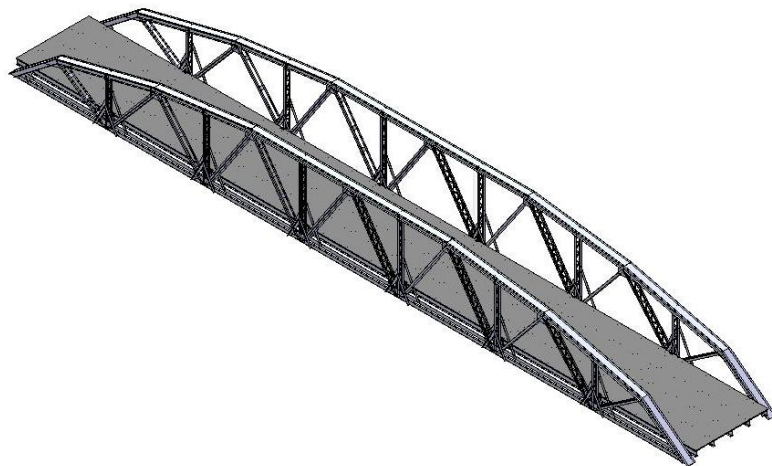


Figure 5 – Isometric view of the bridge (Marques (2015)).

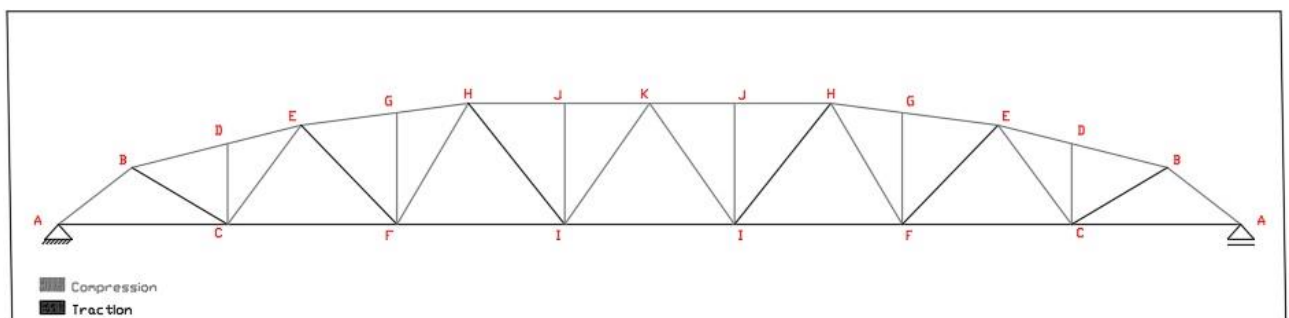


Figure 6 – Bridge overview (adapted from Pereira (2015)).

Table 1 – Internal forces acting in the bridge

Weight [kN]	Half weight [kN]	Bar	Force [kN]	Compression/Traction
1.68	0.84	AB	-81.14	Compression
1.20	0.60	AC	64.35	Traction
0.50	0.25	BC	40.72	Traction
1.46	0.73	BD	-100.90	Compression
0.45	0.22	CD	-1.68	Compression
1.03	0.51	CE	-8.77	Compression
1.21	0.61	CF	24.05	Traction
1.46	0.73	DE	-100.90	Compression
0.63	0.32	EF	24.94	Traction
1.40	0.70	EG	-86.49	Compression
0.63	0.32	FG	-1.72	Compression
1.25	0.62	FH	-4.60	Compression
1.20	0.60	FI	43.77	Traction
1.40	0.70	GH	-86.49	Compression
0.73	0.37	HI	15.89	Traction
1.41	0.70	HJ	-98.04	Compression
1.22	0.61	I-I ²	52.53	Traction
0.69	0.34	IJ	-1.75	Compression
1.41	0.70	JK	-98.04	Compression
1.16	0.58	IK	2.02	Traction

To calculate the normal direct radiation the values of *A* and *B* were given by the table 7-2 in McQuiston, Parker and Spitler (2005) with values 1094 W/m² and 0,186 respectively. *C_N* was based on Liu, Chen and Zhou (2013) experiment, and chosen *C_N* =1.0, the latitude was -22°22'15''N and the local longitude 46°56'38''W being the coordinates of Mogi Guaçu/SP. The standard meridian is Central Standard Time CST 90°.The incident radiation was calculated per hour in the interval from 7:00 a.m. to 5:00 p.m. of the day 203 of the year, July 22th, 2017, the DST is -2hr to Brazil because the chosen day is not in summer. It was considered the hour angle as zero at local solar noon, have its maximum value at sunset, and have its minimum value at sunrise (McQuiston, Parker and Spitler (2005)). The calculations were made using the angle *α* equal to 14° which was the bar angle DE, the bar that has the greatest effort, the incident radiation is shown on Fig 7:

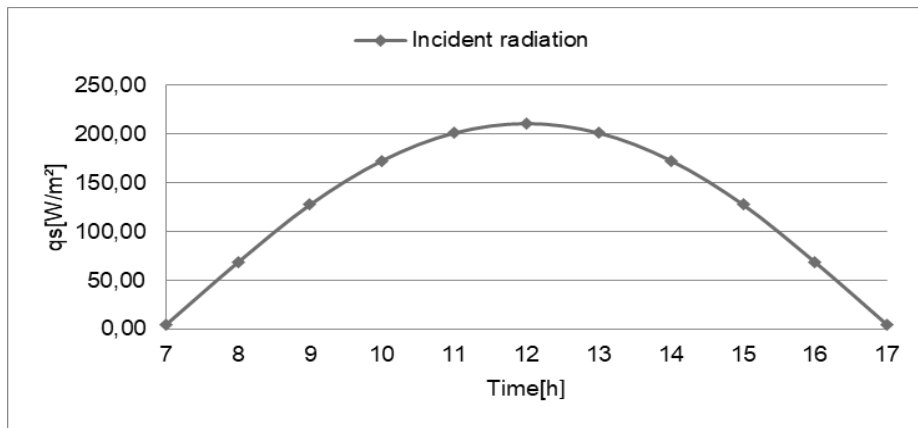


Figure 7 – Solar radiation incident on a non-vertical surface.

The highest incident radiation occurred at 12:00 and is around 211 W/m². In order to approximate the maximum temperature, the emissivity of the trusses is considerate, and the balance equation becomes (Incropera (2008)):

$$q_s = q_l + q_{conv} \tag{22}$$

The ambient temperature can be estimated by Eq. (15) and the results are compared to experimental data. The data were obtained by the National Institute of Meteorology INMET from 7:00 am to 5:00 pm on July 22th, 2017 Fig. 8.

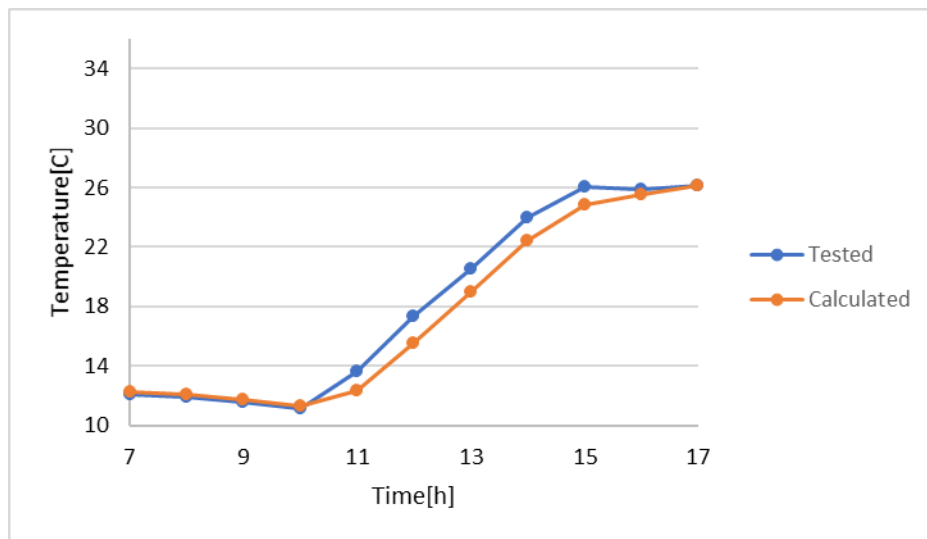


Figure 8 – Ambient temperature model evaluation according to Liu, Chen and Zhou (2013) model.

A comparison and calculation of percent error was made with the maximum difference between the tested and calculated values of temperature, according to Tab. 2:

Table 2 – Difference between measured and calculated temperatures

Hour	Tested temperature (°C)	Calculated temperature (°C)	Absolute error (%)
7	12.1	12.3	3.7
8	11.9	12.0	1.2
9	11.6	11.7	1.3
10	11.1	11.3	0.9
11	13.6	12.4	9.2
12	17.3	15.5	10.1
13	20.5	19.0	7.6
14	24.0	22.4	6.7
15	26.0	24.9	4.4
16	25.9	25.5	1.5
17	26.1	26.2	0.2

To obtain the maximum temperature the coefficient ε was adopted equal to 0.3 and ε_f equal to 0,04 due to the color and material, according Incropera, et al. (2008) and the ground temperature was neglected for the long wave radiation emission. The coefficients C_b , a and b for the convection were based in (McQuiston, Parker and Spitler (2005)) and were equal to 0.84, 2.38 and 0.89, respectively and the average wind speed is equal to 0.2 m/s considering the worst case is windless, for Eq. (16) and Eq. (17) the upper temperature was found by the fixed-point method. The maximum temperature calculated was shown on Fig. 9:

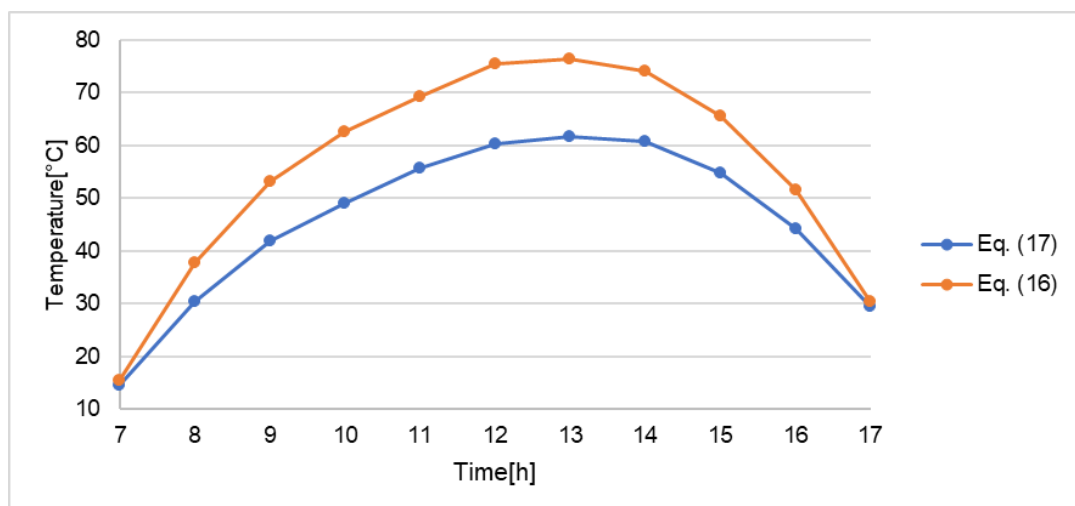


Figure 9 – Calculated temperatures with the different models.

The highest maximum temperatures occurred between 11:00 a.m. and 2:00 p.m., reaching the temperature of 76°C to Eq. (16) and 62°C using Eq. (17) for the convection coefficient, which is relatively close to that measured by Marques (2005).

For the calculation of the thermal stress were used the data of 1:00 p.m. that was the highest as mentioned above, and the DE bar which has the greatest effort. The linear expansion coefficient was $1.2 \times 10^{-5} \text{ } ^\circ\text{C}^{-1}$ that is the value of steel, the Young modulus equal to 200 GPa (Hibbeler, (2004)), and the cross section area is 6216 mm². The stress results are shown on Tab. 3:

Table 3 – Thermal stresses on DE bar at 12:00

Equation	Compression stress [MPa]	Thermal stress [MPa]	Total stress [MPa]
17	-16,2	-144	-160,2
17	-16,2	-108	-124,2

Buckling was estimated using the Euler equation. The cross section used in the calculation was the DE bar, and was shown on figure 10:

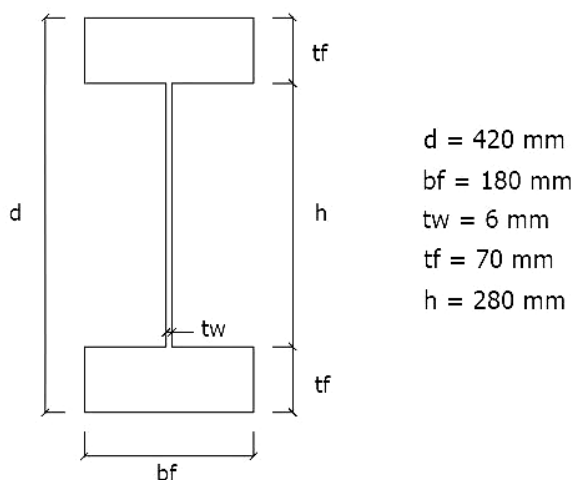


Figure 10 – DE bar cross section.

The critical load was around 2434 kN which is significantly higher than the sum of the loads due to the elements weight and accidental loads. For the calculation, the bar was considered one end fixed and the other end free to move laterally, being $K = 2.0$, L was the length of DE bar being 5,252m and the moment of inertia was found in the smallest direction, which has the highest tendency to deform in relation to the load.

CONCLUSIONS

The solar irradiation has significant effect in the temperature and stresses in steel structures. This work used different models to evaluate the temperature and stress variation. The case study was a steel structure located in Brazil, Mogi Guaçu/SP. The results calculated by the different convection models (Eq. (16) and Eq. (17)), showed the maximum temperature calculated was around 76°C and 62°C which means 375% and 281% higher than ambient temperature. The temperature variation was around 60°C, and 45°C considering a windless day, that is the worst case. The bar under most compression load was 16,2 MPa and the load with the thermal variation calculated was around 889% higher than the compression load to Eq. (16) and 667% to Eq. (17). The bridge is old and the factor of safety is relatively high. Future works can use these models in the design of metallic structures and use a smaller factor of safety in order to reduce the material used in the project.

REFERENCES

- Danosio, J. P., 2005, “Física (Arquitetura)”, Instituto Nacional de Física de São Carlos, São Carlos.
- Hibbeler, R. C., 2004, “Resistencia dos materiais”, São Paulo: Person Prentice Hall.
- Hongo, L., Zhihua C., Ting, Z., 2013, “Investigation on temperature distribution and thermal behavior of large span steel structures considering solar radiation”, Advanced Steel Construction., Vol 9, N1, pp 41-58.
- Incropera, F. P. et al., 2008, “Fundamentals of heat and mass transfer”, Ed. LTC, Rio de Janeiro, 645p.
- Kordun, O.I., 2015, “Influence of solar radiation on temperature increment of sheet steel structures”, Archives of Civil

Engineering., Vol. LXI, pp. 90.

McQuiston, F. C., Parker, J. D., Spitler, J. D., 2005, "Heating, ventilating, and air conditioning analysis and design, USA, John Wiley and Sons.

Pereira, R. F. G., 2015, "Redimensionamento e comparação da ponte metálica de pedestre de Mogi Guaçu utilizando conceitos de tratamentos térmicos", Mogi Guaçu/SP, 60p.

Ricardo, G. M. O., 2015, "Influência da radiação térmica sobre estruturas metálicas", Mogi Guaçu/SP, 80p.

RESPONSIBILITY NOTICE

The authors are the only responsible for the printed material included in this paper.